Sobh *et al. Beni-Suef Univ J Basic Appl Sci* (2023) 12:20
https://doi.org/10.1186/s43088-023-00356-x

Beni-Suef University Journal of Basic and Applied Sciences

RESEARCH

Open Access

Turning parameters optimization for TC21 Ti-alloy using Taguchi technique

Arafa S. Sobh[1*], Esraa M. Sayed[2], Azzz F. Barakat[3] and Ramadan N. Elshaerr[4]

Abstract

Background The development of materials fabrication is an important trend in materials engineering. TC21 Ti-alloy is one of these materials' trends. Investigations of different characteristics of TC21 Ti-alloy such as weldability, formability, and machinability will consume a large number of specimens. This work aims to study the machinability characteristics of TC21 Ti-alloy. The minimum number of experimental trials and optimal cutting conditions will be obtained by applying the orthogonal array (OA) L9 Taguchi technique. To achieve this aim, experimental work will be conducted under three varying cutting parameters, each one of them with three levels: cutting speeds (V) of 80, 100, and 120 m/min, feed rates (f) of 0.05, 0.10, and 0.15 mm/rev, and cutting depth (a) of 0.2, 0.4, and 0.6 mm.

Results The results revealed that the cutting depth and cutting speed with percentages contribution of 40.8% and 48.6%, respectively, are the most significant parameters of surface roughness and wear of the tool insert. However, the least significant parameters are cutting speed and feed rate with percentages contribution of 20.2% and 2.3%, respectively.

Conclusions Minimum surface roughness at V = 80 m/min, f = 0.10 mm/rev, and a = 0.4 mm is 0.16 µm, and maximum surface roughness at V = 80 m/min, f = 0.15 mm/rev, and a = 0.6 mm is 0.72 µm. Minimum tool wear at V = 100 m/min, f = 0.15 mm/rev, and a = 0.2 is 187.770 µm, and the maximum tool wear at V = 80 m/min, f = 0.10 mm/rev, and a = 0.4 mm is 274.896 µm.

Keywords TC21Ti-alloy, Machinability, Tool wear, Surface roughness, Taguchi

1 Background

The most common titanium alloys are Ti555.3, Ti 6Al 4 V, and TC21. Recently, titanium alloys have become more popular as they are used in many applications. Particularly in aerospace, military, automotive, biomedical, and communications engineering, because titanium alloys have a high strength-to-weight ratio and good corrosion resistance. Whereas their high chemical reaction with cutting tool material and low thermal conductivity leads to making titanium alloys difficult to machine, thus these alloys require special preparation for machining processes [1–4].

The TC21 Ti-alloy is a modern generation of titanium alloys with the chemical composition (Ti–6Al–3Mo–2Zr–2Sn–2Nb–1.5Cr–0.1Si), and its microstructure has two-phase (α + β). It possesses high hardness, tensile strength, toughness, good plasticity, fatigue, and creep resistance. However, it has poor tribological properties.

Although there is a wide spread of TC21 applications, they are limited to military applications; aircraft, spacecraft, bicycles, biomedical devices, jewelry, highly stressed components such as connecting rods on expensive sports cars, and some premium sports equipment

*Correspondence:
Arafa S. Sobh
Arafa_sobh@h-eng.helwan.edu.eg
[1] Mechanical Engineering Department, Faculty of Engineering, Helwan University, 5Th Settlement, Cairo, Egypt
[2] Mechanical Engineering Department, Faculty of Engineering, Helwan University, El-Zahraa Misr El-Qadima, Cairo, Egypt
[3] Mechanical Engineering Department, Faculty of Engineering, Helwan University, El-Maadi, Cairo, Egypt
[4] Mechanical Engineering Department, Tabbin Institute for Metallurgical Studies, Helwan, Cairo, Egypt

and consumer electronics [5–7], because the drawbacks of TC21 Ti-alloy are the high cost of both raw materials and the obstacle of machining, which leads to low efficiency, fast tool wear, and low surface quality. The machining technicality of this alloy needs to be inspected deeply. To inspect the machining operation of TC21 Ti-alloy, a group of turning experiments was done [8–10].

In the last decades, there has been a big problem in selecting machining parameters, as the researchers selected the parameters according to the latest studies using full factorial, which is very costly and consumes more time. In recent years, there has been progressed in parameters selection techniques, to get the optimum parameters of machining. There are several techniques, such as response surface methodology (RSM), Taguchi, ANOVA, and artificial neural network (ANN) [11]. With the development of new materials such as TC21 Ti-alloy, there is a demand for studying many fields about it, such as the attitude of TC21 Ti-alloy in metal forming, heat treatment influence on microstructure and cutting parameters, and the big problem of TC21 Ti-alloy is the machinability, such as turning, milling, and turn milling. Over recent decades, there is now a lot of interest in studying the laser surface treatment [12, 13] and oxidation of TC21 Ti-alloy [14, 15]. However, there are no in-depth descriptions of the study of the machinability characteristics of TC21 Ti-alloy.

TC21 Ti-alloy has better tensile strength and toughness than Ti–6Al–4V and Ti 555.3 alloys. This alloy is now used in more aircraft and military applications. However, the main drawback of this alloy is that it has cutting difficulty. That led to many machining studies having been done on it. Many researchers have performed turning operations on this alloy with varying levels of machining parameters like feed rate, cutting depth, and cutting speed, employing the Taguchi technique to get the optimum conditions of turning parameters [16–18]. In addition to fractional factorial using the Taguchi technique, other scientists used the full factorial technique [19, 20]. The difference between full factorial and fractional factorial (Taguchi technique) is that full factorial applies a complete combination of trials (full array), while the Taguchi applies a sub-array which saves a number of samples, cost, and time. Therefore, the results reported that the data analysis (DA) during the present study indicates that the Taguchi technique is more proper for analyzing the machinability of "difficult-to-cut" materials than the full factorial.

Besides the Taguchi technique, there is the response surface technique to optimize the parameters of machining operations. Other researchers used the prediction modeling of surface roughness as reported by the response surface technique to investigate. They revealed that the objective of optimization is to obtain the maximum removal rate of material. A genetic algorithm and response surfaces were implemented to optimize the machining parameter's influence on surface roughness. By surface roughness tester, the surface roughness values have been obtained from the average of three values on the workpiece surface [21].

In the metal forming field, some researchers studied the behavior of this alloy using isothermal tensile tests. They found from stress–strain curves that there is a reverse relationship between the flow stress and temperature, and a straight relationship between the flow stress and rate of strain [22]. While other researchers studied the same relationship but in hot deformation using high temperature tensile tests and constitutive modeling, they discovered a reverse relationship between the flow stress and rate of strain, as well as a direct relation between the stress and **strain** [23].

Some studies have been performed in machining field to inspect the tool microstructure influence and variation of tool rake angles on the machining technicality of TC21 Ti-alloy. This is done using finite element analysis to develop the cutting effectiveness of this alloy. In addition, 3D finite element analysis and the Johnson–Cook (JC) technique are used to simulate the turning operation of this alloy. The consequences revealed that **decreased** serration of scrapes and wear of the tool insert and improved machining effectiveness of this alloy were obtained by varying tool rake angles. Finally, 3D simulation is very narrow with experimental results [24–27].

Lei and Xuedao investigated the turning process of the TC21 Ti-alloy, so they also studied the influence of some important turning parameters (cutting speed, feed speed, depth of cut, and rake angle) on cutting force and chip morphology but with other levels of parameters. The experimental conditions are set as follows: Feed speed is 0.01, 0.02, 0.03, and 0.04 mm/rev, spindle speed is 120, 180, 240, and 300 m/min; depth of cut is 0.1, 0.2, 0.3, and 0.4 mm, rake angles are 0°–15° with interval of 5°, and clearance angles are 15°. It is followed by utilizing 3D simulation using the software ABAQUS. The results of experiments proved that the rake angle of tool has the obvious impact on the chip morphology and larger rake angle can decrease the extent of chip serration. The high cutting speed is more suitable to cutting the alloy, and the results of simulation were well validated by the comparison of chip formation and cutting forces with the results of experiments [28].

Xu and Hongbing investigated the impact of tool angles on cutting force and residual stress in the oblique cutting of TC21 Ti-alloy. The experimental conditions are set as follows: Spindle speed is 4000 rev/min, depth of cut is 0.2 mm, rake angles are 5°–20° with interval of 5°, clearance angles

are 5°–20° with interval of 5°, and inclination angle is 20°. Subsequently, 3D finite element model (FEM) of oblique cutting during simulation Johnson–Cook material law has been adopted. The results viewed that the influence of tool geometrical parameters on the turning forces of TC21 Ti-alloy has been analyzed by the simulation and test. In the same cutting parameters, the turning force of simulation agreed well with the turning force of experiment [29].

Xiaohua and Xiongying verified the influence of tool texture on machining of titanium alloy TC21: firstly, by simulation method using 3D orthogonal finite 27 element model (OFEM) and secondly, comparing the results by experiment works. Resulting simulations indicated that tool texture demonstrably improves the machinability of TC21 alloy, reducing cutting temperature and cutting force. Finally, the testing confirmed that chip serration and tool wear can be reduced using textured tools. Overall, this research successfully proves that textured tool can clearly improve the machinability of TC21 Ti-alloy [30].

Liying et.al examined the surface roughness of TC21 Ti-alloy by two different ways: The first method was experimentally using orthogonal test of TC21 Ti-alloy with high-speed turning parameters. The experimental conditions are set as follows: Feed speeds are 0.05, 0.1, 0.15, 0.20, 0.25 mm/rev, spindle speeds are 80,100,120,140,160 m/min, and cutting depths are 0.2, 0.4, 0.6, 0.8,1 mm. The second method was mathematically optimized using genetic algorithm. The results concluded that the optimal combination of cutting parameters is v2 f1 a2. The corresponding experiment parameters are v2 = 100 m/min, f1 = 0.05 mm/r, a2 = 0.4 mm, and the surface roughness is Ra = 0.4240 dB [21].

Due to its exceptional mechanical qualities, titanium and its alloys are widely used in a variety of applications. The high strength, low heat conductivity, and long chips produced by typical machining operations in titanium alloys, however, make them difficult to machine and contribute to their poor machinability. New machining techniques and advanced have been used to improve these alloys machinability. One of these advanced machining methods is ultrasonic vibration assisted turning (UVAT) [31–33]. Their outstanding corrosion resistance, high strength, and low weight lead to that titanium alloys are widely employed in the aerospace, marine, medical, and chemical processing industries. However, due to their great strength and low heat conductivity, these alloys are extremely difficult to machine using standard machining techniques like conventional turning [34].

In this research paper, the influence of turning parameters was optimized by the Taguchi technique using Minitab 19 software to determine the number of experiments and get the optimum conditions for low surface roughness and low tool insert wear, subsequently applying the ANOVA technique to get the most significant parameters. The machining of TC21 Ti-alloy requires the greatest setting; therefore, in this work, a tungsten carbide-coated cutting tool (DCMT 11 T 304-NF NS 4125) is used.

2 Methodology

2.1 Material composition and preparation

The experimental material used is TC21 Ti-alloy for chemical composition as shown in Table 1. Its mechanical properties are very high tensile strength and toughness (even at extreme temperatures), and it has a microstructure of two phases ($\alpha+\beta$) of titanium alloy. Figure 1 displays the microstructure of this alloy. The dimensions of the samples are 33 mm in diameter and a length of **110** mm**.**

2.2 Method

The experimental equipment is the GOOD WAY. For the ultimate CNC machining power (3000 rpm maximum spindle speed), cutting tools are indexable tungsten-coated carbide (DCMT 11 T 304-NF NS 4125) with a

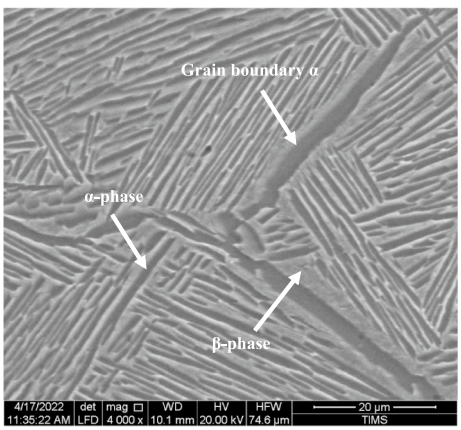

Fig. 1 TC21 Ti-alloy microstructure

Table 1 Chemical composition of TC21 Ti-alloy

Composition	Al	Mo	Zr	Sn	Nb	Cr	Si	Fe	C	N	H	O	Ti
Weight percent/Wt.%	6.39	2.74	2.31	2.21	2.02	1.64	0.11	0.04	0.04	0.04	0.003	0.13	Balance

nose radius of 0.4 mm because the coated tungsten carbide is most suitable insert to machine difficult to cut materials like TC21. The experiments were repeated three times to take the average for each response. The surface roughness of the TC21 Ti-alloy was measured by the DIAVITE DH-5 tester for surface roughness. Each surface roughness value is the average value of the surface roughness (Ra) measured at the three positions on the surface. The experiments of three factors (feed rate, cutting speed and cutting depth) with three levels are shown in Table 2a. To study the worn surface of the tool wear, scanning electron microscopy (SEM) was used to examine some selected samples from the applied experiments (one from each parameter) and take the maximum depth of wear for each sample.

2.2.1 Design of experiments using Taguchi technique

A fractional factorial design using the Taguchi technique is applied to optimize experiments number. The experiment number was conducted using the orthogonal array L9 for three parameters (speed of cut, feed rate, and cutting depth) at three levels (level 1, level 2, and level 3). Table 2 shows the levels and orthogonal array of parameters, respectively.

Based on the literature review, it can be observed that most researchers used cutting speeds for machining titanium alloys greater than 54 m/min. Considering references (3,18,21 and 27) that used cutting speed levels such as (80,100,120,140,160.... etc.) m/min for machining titanium alloys, in addition to cutting speeds range, there are small cutting depths in range 0.1: 1 mm and feed rates in range 0.05:0.25 mm/rev, because titanium alloys are used in tiny applications. we tried to use the same values and applied Taguchi technique to arrange the effect of each parameter on our response.

Optimization of parameters of any process is the main procedure in the Taguchi technique to achieve the improvement of quality performance and a reduction in experimental turning cost. Optimization of the parameters of the process by the Taguchi technique leads to obtaining the optimal parameters that are insensitive to environmental conditions and noise. The Taguchi method defines a loss function that is utilized to calculate the deflection between the value from the experimental work and the desired value from the Taguchi technique. This loss function is further transferred into a signal-to-noise (S/N) ratio.

The signal-to-noise (S/N) ratio depends on the category of the required response. There are three equations to calculate the signal-to-noise ratio (S/N). Smaller is better (SB) as shown in Eq. (1), nominal is better (NB) as shown in Eq. (2), and larger is better (LB) as presented in Eq. (3) [35, 36].

Smaller is the better (minimize):

$$S/N = \eta = -10 \log \left(\sum \left(y^2 \right) / n \right) \quad (1)$$

Table 2 (a) Parameters and their levels of the work, (b) the orthogonal array L9 by Taguchi technique

(a)

Factors	Level (1)	Level (2)	Level (3)
Speed of cut V(m/min)	80	100	120
Feed rate f (mm/rev)	0.05	0.10	0.15
Cutting depth a (mm)	0.2	0.4	0.6

(b)

Exp. No	Speed of cut (V)	Feed rate (f)	Cutting depth (a)
1	1	1	1
2	1	2	2
3	1	3	3
4	2	1	3
5	2	2	1
6	2	3	2
7	3	1	2
8	3	2	3
9	3	3	1

Nominal is best

$$S/N = \eta = 10\log 10\left(\frac{Y^{-2}}{S^2}\right) \quad (2)$$

Larger is better (maximize)

$$S/N = \eta = -10\log 10\left(\sum\left(\frac{1}{Y^2}\right)/n\right) \quad (3)$$

Table 3 Experimental results of surface roughness Ra

Experimental serial number	Speed of cut V (m/min)	Feed rate f (mm/rev)	Depth of cut a (mm)	Surface roughness Ra (μm) Mean
1	80	0.05	0.2	0.296667
2	80	0.10	0.4	0.160000
3	80	0.15	0.6	0.720000
4	100	0.05	0.4	0.263333
5	100	0.10	0.6	0.433333
6	100	0.15	0.2	0.523333
7	120	0.05	0.6	0.646667
8	120	0.10	0.2	0.416667
9	120	0.15	0.4	0.563333

Table 4 Experimental results for wear of tool insert

Experimental serial number	Cutting speed V (m/min)	Feed rate f (mm/rev)	Cutting depth a (mm)	Tool wear Ymax (μm) Mean
1	80	0.05	0.2	221.697
2	80	0.10	0.4	274.896
3	80	0.15	0.6	268.570
4	100	0.05	0.4	229.129
5	100	0.10	0.6	226.584
6	100	0.15	0.2	187.770
7	120	0.05	0.6	263.200
8	120	0.10	0.2	235.300
9	120	0.15	0.4	257.071

where

S/N is signal-to-noise ratio

n is the number of experiments

$\overline{Y}$ is the average of the experiment results

Y is the experiment result.

S^2 is the standard deviation of the experiment results.

2.2.2 Experimental measurements

We used a standard international block to make a calibration stage for surface roughness tester (DIAVITE DH-5 tester) and scanning electron microscope (SEM) to make sure the accuracy of these instruments. For surface roughness results, the experiments were repeated three times to take the average for each response. The measurements of surface roughness are displayed in Table 3.

To investigate the wear surface of tool wear, scanning electron microscopy (SEM) was used to examine several selected samples (one from each parameter) from the applied experiments and determine the maximum wear depth of each sample. The measurements of tool wear are displayed in Table 4.

3 Results

3.1 Results of surface roughness

3.1.1 Signal-to-noise ratio analysis

In this work, smaller surface roughness is an indication of better effectiveness. Therefore, to get the optimum machining parameters, the smaller the better it was selected for surface roughness. The highest signal-to-noise ratio (S/N) of the machining parameter levels indicates an optimum level [16, 21]. The results of surface roughness and the calculated (S/N) ratio of each parameter level are represented in Table 5. From the S/N ratios, it is obtained that the optimum parameters for surface roughness are at experiment no. 2 (V1 f 2 a2), which represents the highest S/N ratio. The parameters for this experiment are V= 80 m/min, f= 0.05 mm/rev, and a = 0.4 mm. The optimum parameters are presented in Table 6.

Table 5 Experimental results of surface roughness Ra and S/N ratio

Experimental serial number	Speed of cut V (m/min)	Feed rate f (mm/rev)	Depth of cut a (mm)	Surface roughness Ra (μm) Mean	Ra S/N (μm)
1	80	0.05	0.2	0.296667	10.5546
2	80	0.10	0.4	0.160000	15.9176
3	80	0.15	0.6	0.720000	2.8534
4	100	0.05	0.4	0.263333	11.5899
5	100	0.10	0.6	0.433333	7.2636
6	100	0.15	0.2	0.523333	5.6244
7	120	0.05	0.6	0.646667	3.7864
8	120	0.10	0.2	0.416667	7.6042
9	120	0.15	0.4	0.563333	4.9847

Table 6 Optimum process parameters

Exp. No	Process Parameters	Surface roughness (μm)
2	V1 f2 a2	0.16

Table 8 Optimum process parameters

Exp. No	Process Parameters	Tool wear (μm)
6	V2 f3 a1	187.770

3.2 Results of tool wear

3.2.1 Signal-to-noise ratio analysis

In this work, smaller tool wear is an indication of better effectiveness. Therefore, to obtain the optimum parameters of machining, the smaller the better it was selected for tool wear. The highest signal-to-noise ratio (S/N) of the machining parameter levels indicates an optimal level [16, 21]. The results of tool wear and the calculated (S/N) ratio of each parameter level are represented in Table 7. It displays the measured values of tool wear and the calculated S/N ratio for the nine experiments on TC21. From the S/N ratios, it is obtained that the optimum parameters for surface roughness are at experiment no. 6 (V2 f 3 a1), which represents the highest S/N ratio. The parameters for this experiment are V= 100 m/min, f= 0.15 mm/rev, and a= 0.2 mm. The optimum parameters are presented in Table 8.

4 Discussion

4.1 Discussion of surface roughness results

4.1.1 Signal-to-noise ratio response

The average S/N ratio is calculated for each parameter to arrange the cutting parameters according to the most significant. For example, a sample calculation as shown through equations (4:6) for factor V (cutting speed) is [37]:

$$\mathrm{SNv1} = (10.5404 + 15.9176 + 2.8494)/3 = 9.76915 \quad (4)$$

Table 9 S/N response and the delta value of Ra for each parameter

Level	V	f	A
1	9.775	8.644	7.928
2	8.159	10.262	10.831
3	5.458	4.487	4.634
Delta	4.317	5.774	6.196
Rank	3	2	1

$$\mathrm{SNv2} = (11.4813 + 7.2384 + 5.6177)/3 = 8.11250 \quad (5)$$

$$\mathrm{SNv3} = (3.7848 + 7.3041 + 4.9535)/3 = 5.34745 \quad (6)$$

The effect of this factor is calculated by determining the range:

$$\Delta = \mathrm{SNVmax.} - \mathrm{SNVmin.} = 9.76915 - 5.34745 = 4.422$$

From the calculations, as shown in the previous equations (4:6), Table 9 will be obtained. In this study from Table 9, it is found that the cutting depth parameter has the largest difference between its levels and leads to having a high effect on the experiment response (surface roughness), whereas the cutting speed parameter has a low influence on the experiment response (surface roughness).

Table 7 Experimental results for wear of tool insert and S/N ratio

Experimental serial number	Cutting speed V (m/min)	Feed rate f (mm/rev)	Cutting depth a (mm)	Tool wear Ymax (μm) Mean	Ymax S/N (μm)
1	80	0.05	0.2	221.697	−46.9152
2	80	0.10	0.4	274.896	−48.7834
3	80	0.15	0.6	268.570	−48.5811
4	100	0.05	0.4	229.129	−47.2016
5	100	0.10	0.6	226.584	−47.1046
6	100	0.15	0.2	187.770	−45.4725
7	120	0.05	0.6	263.200	−48.4057
8	120	0.10	0.2	235.300	−47.4324
9	120	0.15	0.4	257.071	−48.2011

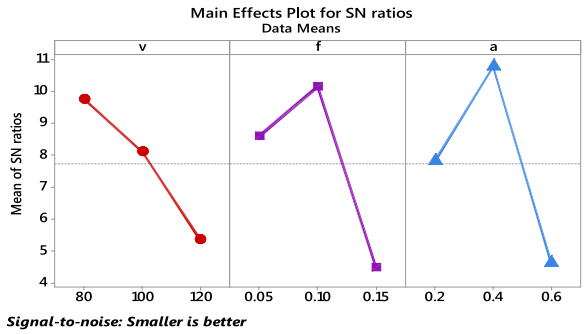

Fig. 2 Mean of S/N ratio for Ra

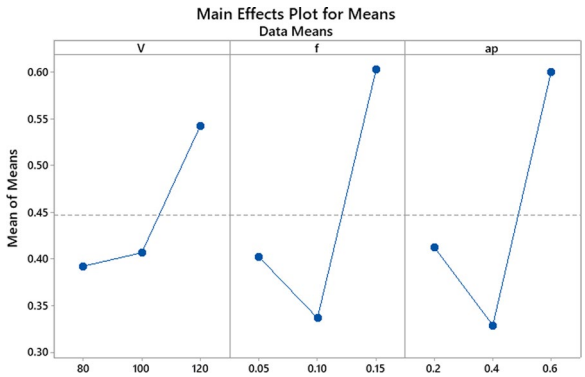

Fig. 3 Main effects plot for means for Ra

4.2 Diversity of parameters with signal-to-noise ratio (S/N)

The following figure shows the variation for all parameters with signal-to-noise ratio. From Table 9, it is seen that the delta values for parameters V, f, and a are 4.422, 5.680, and 6.160, respectively. The delta value for each parameter is plotted in Fig. 2.

But from Fig. 3, it is shown that the surface roughness value is in direct relation with the cutting speed parameter. When the depth of cut and feed rate rise, it lowers from level one to level two and subsequently climbs from level two to level three. It is noticed that there is a long variation between the levels of two parameters mentioned above. Consequently, the mentioned two parameters occupy the first two affected parameters in the machining process [16, 21].

Table 11 S/N response and the delta value of Ymax for each parameter

Level	V	f	a
1	−48.0932	−47.51	−46.61
2	−46.5929	−47.77	−48.06
3	−48.0131	−47.42	−48.03
Delta	1.50	0.36	1.46
Rank	1	3	2

4.3 Analysis of variance (ANOVA)

ANOVA was used to determine the influence of cutting speed, feed rate, and cutting depth on surface roughness. Table 10 displays the consequences of the investigation at a 95% confidence level. The depth of cut is the most significant parameter of surface roughness, with a percent contribution of 40.8%. In addition, the least significant parameter is the cutting speed with a percent contribution of 20.2%.

4.4 Discussion of tool wear results

4.4.1 Tool wear (Signal-to-noise ratio response)

The average S/N ratio is calculated for each factor to arrange the parameters according to the most significant. For example, a sample calculation as shown through equations (7:9) for factor V (cutting speed) is [37]:

$$SNv1 = (-46.9152 - 48.7834 - 48.5811)/3 = -48.0932 \quad (7)$$

$$SNv2 = (-47.2016 - 47.1046 - 45.4725)/3 = -46.5929 \quad (8)$$

$$SNv3 = (-48.4057 - 47.4324 - 48.2011)/3 = -48.0131 \quad (9)$$

The effect of this factor is calculated by determining the range:

Table 10 ANOVA optimization

Source	Degree of freedom (DOF)	Sum of squares (SS)	Adj (SS)	Adj (MS)	F	*P*-Value	Percent contribution (PC) %	Remarks
V	2	28.540	28.540	14.270	14.50	0.065	20.18	Insignificant
F	2	53.235	53.235	26.617	27.05	0.036	37.65	Significant
A	2	57.667	57.667	28.834	29.30	0.033	40.78	Significant
Residual error	2	1.968	1.968	0.9841				
Total	8	141.410						

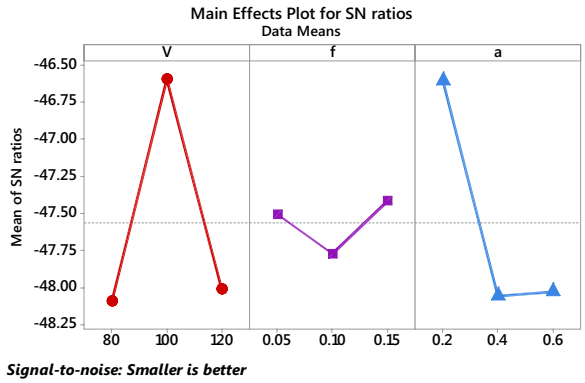

Fig. 4 Mean of S/N ratio for Ymax

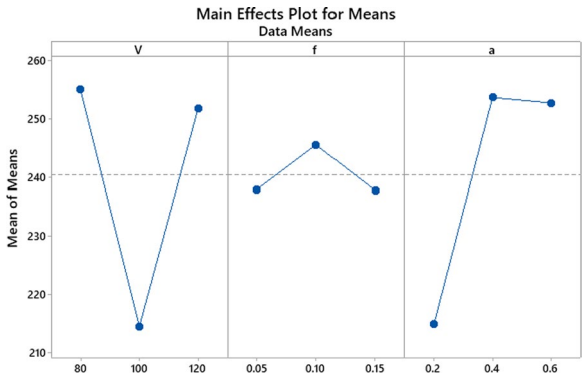

Fig. 5 Main effects plot for means

$$\Delta = \text{SNVmax.} - \text{SNVmin.} = -46.5929 - (-48.0932) = 1.50$$

From the calculations, as shown in the previous equations (7:9), Table 11 will be obtained. In this study from Table 11, it is seen that the cutting speed parameter has the largest difference between its levels and leads to having a high effect on the experiment response (tool wear), whereas the feed rate parameter has a low effect on the experiment response (tool wear).

4.5 Diversity of parameters with signal-to-noise ratio (S/N)

The following figure shows the variation for all parameters with signal-to-noise ratio. From Table 11, it is seen that the delta values for parameters V, f and a are 1.50, 0.36 and 1.46, respectively. The delta value for each parameter is plotted in Fig. 4.

From Fig. 5, it is shown that the tool wear value decreases from level one to level two with the cutting speed parameter. When the feed rate and depth of cut increase, it rises from level one to level two and then falls from level two to level three. It is noticed that there is a long variation between the levels cutting speed and depth of cut. Consequently, the two parameters occupy the first two affected parameters on the machining process [38].

4.6 Analysis of variance (ANOVA)

ANOVA was used to determine the influence of cutting speed, feed rate and cutting depth on tool wear. Table 12 displays the consequences of the investigation at a 95% confidence level. It can be concluded that the most significant parameter for tool insert wear is the cutting speed, and its percent contribution is 48.6%. In addition, the least significant parameter is the feed rate with a percent contribution of 2.3%.

4.7 Tool wear mechanism

To inspect the technicality of tool wear in the turning of TC21 alloy, the flank face for tool inserts was investigated using a scanning electron microscope (SEM) to measure the tool wear height for each experiment to be optimized using the Taguchi technique as displayed in Table 4. Figure 6 illustrates the scanned image for all experiments. In the turning experiments of TC21, cutting speed has the greatest influence on tool wear during turning tests.

5 Conclusions

According to the prediction model of surface roughness of TC21 Ti-alloy and the prediction model of tool wear of tool insets, it is found that:

Table 12 ANOVA optimization for tool wear

Source	Degree of freedom (DOF)	Sum of squares (SS)	Adj (SS)	Adj (MS)	F	*P*-Value	Percent contribution (PC) %	Remarks
V	2	4.2743	4.2743	2.13715	25.83	0.037	48.622	Significant
F	2	0.2049	0.2049	0.10244	1.24	0.447	2.331	Insignificant
a	2	4.1460	4.1460	2.07299	25.05	0.038	47.16	Significant
Residual error	2	0.1655	0.1655	0.08275			1.883	
Total	8	8.7907						

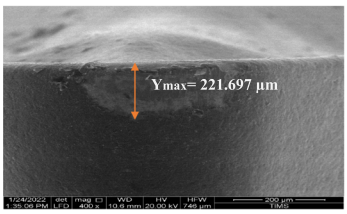

Experiments no.1(V=80 m/min, f=0.05 mm/rev, a=0.2mm) and Ymax=221.697 µm

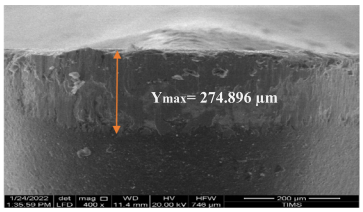

Experiment no.2 (V=80 m/min, f=0.10, a=0.4 mm) and Ymax=274.896 µm

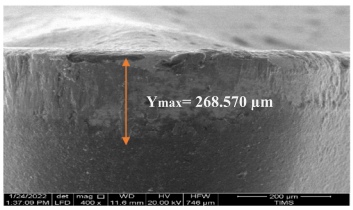

Experiment no.3 (V=80 m/min, f=0.15 mm/rev, a=0.6 mm) and Ymax=268.570 µm

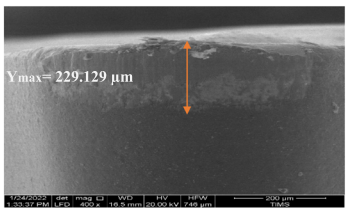

Experiment no.4 (V=100 m/min, f=0.05 mm/rev, a=0.4 mm) and Ymax=229.129 µm

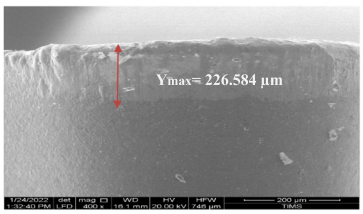

Experiment no.5 (V=100 m/min, f=0.10 mm/rev, a=0.6 mm) and Ymax=226.584 µm

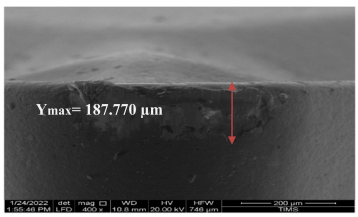

Experiment no.6 (V=100 m/min, f=0.15 mm/rev, a=0.2 mm) and Ymax=187.770 µm [optimal experiment]

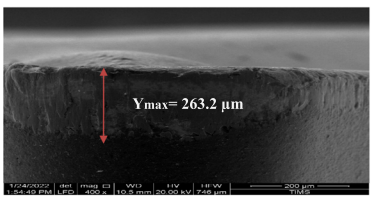

Experiment no.7 (V=120 m/min, f=0.05 mm/rev, a=0.6 mm) and Ymax=263.2 µm

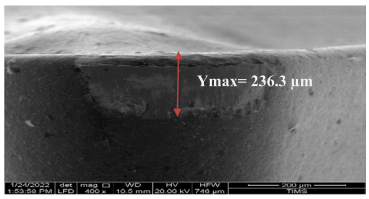

Experiment no.8 (V=120 m/min, f=0.10 mm/rev, a=0.2 mm) and Ymax=235.3 µm

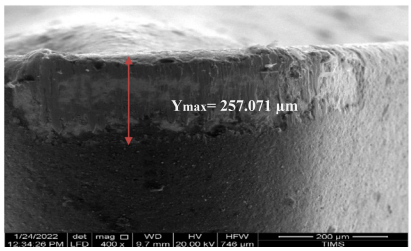

Experiment no.9 (V=120 m/min, f=0.15 mm/rev, a=0.4 mm) and

Fig. 6 SEM images of the flank face

1. The lowest surface roughness is at the highest signal-to-noise ratio at optimal conditions at experiment no. 2. The optimum parameters of machining (V = 80 m/min, f = 0.1 mm/rev, and a = 0.4 mm) with Ra = 0.16 μm.
2. The most significant parameter in surface roughness is the cutting depth with a percentage contribution of 40.8%.
3. The least significant parameter in surface roughness is the cutting speed with a percentage contribution of 20.2%.
4. The lowest tool wear is at the highest signal-to-noise ratio at optimal conditions in experiment no. 6. The optimum parameters of machining (V = 100 m/min, f = 0.15 mm/rev, and a = 0.2 mm) with Y = 187.77 μm.
5. The most significant parameter in tool insert wear is the cutting speed with a percentage contribution of 48.6%.
6. The least significant parameter in tool wear is the feed rate with a percentage contribution of 2.3%.

Abbreviations

SEM	Scanning electron microscope
V	Cutting speed (m/min)
f	Feed rate (mm/rev)
a	Depth of cut (mm)
Ra	Mean of surface roughness (dB)
Ymax	Tool wear depth (μm)
ANOVA	Analysis of variance
SNR or S/N ratio	Signal-to-noise ratio
SS	Sum of square

Acknowledgements
Not applicable.

Author contributions
All authors contributed in this study. AB helped in collecting data. RE helped in scanning process. AS helped in data analysis after ES made the experiments . All authors read and approved the final manuscript.

Funding
There has been no funding for this study.

Availability of data and material
All data generated or analyzed during this study are included in this published article and it's supplementary information files.

Declarations

Ethics approval and consent to participate
Not applicable.

Consent for publication
Not applicable.

Competing interests
The authors declare that they have no competing interests.

Received: 20 October 2022 Accepted: 1 February 2023
Published online: 16 February 2023

References

1. Khanna N, Sangwan KS (2013) Machinability study of α/β and β titanium alloys in different heat treatment conditions. Proc Inst Mech Eng Part B: J Eng Manuf 227(3):357–361. https://doi.org/10.1177/0954405412469509
2. Zhaoju Z, Sun J (2016) Investigation on the influence of tool wear upon chip morphology in end milling titanium alloy Ti6Al4V. Int J Adv Manuf Technol 83:1477–1485. https://doi.org/10.1007/s00170-015-7690-1
3. Balaji JH, Krishnaraj V, Yogeswaraj S (2013) Investigation on high speed turning of titanium alloys. Proc Eng 64:926–935. https://doi.org/10.1016/j.proeng.2013.09.169
4. Elshaer RN, Abdelhameed M, Ibrahim KM, El-Shennawy M, Sobh A (2022) Static and fatigue characteristics of heat-treated Ti–6Al–3Mo–2Zr–2Sn–2Nb–1.5 Cr–0.1 Si Alloy. Metallogr Microstruct Anal 11(3):443–453. https://doi.org/10.1007/s13632-022-00856-9
5. Yan-lei ZHAO, Bo-long LI, Zhi-shou ZHU, Zuo-ren NIE (2010) The high temperature deformation behavior and microstructure of TC21 titanium alloy. Mater Sci Eng A 527:5360–5367. https://doi.org/10.1016/j.msea.2010.05.076
6. Zhu YC, Zeng WD, Liu JL, Zhao YQ, Zhou YG, Yu HQ (2012) Effect of processing parameters on the hot deformation behavior of as-cast TC21 titanium alloy. Mater Design 33:264–272. https://doi.org/10.1016/j.matdes.2011.07.018
7. Zhi-feng SHI, Hong-zhen GUO, Jin-yang HAN, Ze-kun YAO (2013) Microstructure and mechanical properties of TC21 titanium alloy after heat treatment. Trans Nonferr Metals Soc China 23(10):2882–2889. https://doi.org/10.1016/S1003-6326(13)62810-1
8. Zhang H, Zhao J, Wang F, Zhao J, Li A (2015) Cutting forces and tool failure in high-speed milling of titanium alloy TC21 with coated carbide tools. Inst Mech Eng 229(1):20–27. https://doi.org/10.1177/0954405414526578
9. Elshaer RN (2022) Effect of initial α-phase morphology on microstructure, mechanical properties, and work-hardening instability during heat treatment of TC21 Ti-alloy. Metallogr Microstruct Anal. https://doi.org/10.1007/s13632-022-00840-3
10. Zhi-feng SHI, Hong-zhen GUO, Jin-yang HAN, Ze-kun YAO (2013) Microstructure and mechanical properties of TC21 titanium alloy after heat treatment. Trans Nonferr Met Soc 23:2882–2889. https://doi.org/10.1016/S1003-6326(13)62810-1
11. Raut Y, Bhaskar A (2020) Optimization of parameters to reduce the surface roughness in face milling operation on stainless steel and mild steel work piece applying Taguchi Method. Int J Sci Res Eng Trends 6:202–208. https://doi.org/10.14445/22315381/IJETT-V68I1P202
12. Elshazli AM, Elshaer RN, Hussein AHA, Al-Sayed SR (2021) Laser surface modification of TC21 (α/β) titanium alloy using a direct energy deposition (DED) process. Micromachines 12(7):739. https://doi.org/10.3390/mi12070739
13. Elshaer RN, Elshazli AM, Hussein AHA, Al-Sayed SR (2022) Impact of laser process parameters in direct energy deposition on microstructure, layer characteristics, and microhardness of TC21 alloy. Int J Adv Manuf Technol 121(7):5139–5154. https://doi.org/10.1007/s00170-022-09644-9
14. Ahmed FS, El-Zomor MA, Ghazala MSA, Elshaer RN (2022) Effect of oxide layers formed by thermal oxidation on mechanical properties and NaCl-induced hot corrosion behavior of TC21 Ti-alloy. Sci Rep 12(1):19265. https://doi.org/10.1038/s41598-022-23724-6
15. Ahmed FS, El-Zomor MA, Abo Ghazala MS, Elshaer RN (2022) Influence of α-phase morphology on mechanical characteristics, cycle oxidation, and hot corrosion behavior of Ti-6Al-3Mo-2Nb-2Zr-2Sn-1.5 Cr alloy. Metallogr Microstruct Anal 11(5):746–760. https://doi.org/10.1007/s13632-022-00884-5
16. Shahebrahimia SP, Dadvandb A (2013) Optimization of cutting parameters for turning operation of titanium alloy Ti-6Al-4V material workpiece using the Taguchi method. Adv Mater Res 685:57–62. https://doi.org/10.4028/www.scientific.net/AMR.685.57

17. Hasçalık A, Çaydaş U (2008) Optimization of turning parameters for surface roughness and tool life based on the Taguchi method. Int J Adv Manuf Technol 38:896–903. https://doi.org/10.1007/s00170-007-1147-0
18. Kumar SR, Kulkarni SK (2017) Analysis of hard machining of titanium alloy by Taguchi method. Mater Today Proc 4(10):10729–10738. https://doi.org/10.1016/j.matpr.2017.08.020
19. Kechagias JD, Aslani KE, Fountas NA, Vaxevanidis NM, Manolakos DE (2020) A comparative investigation of Taguchi and full factorial design for machinability prediction in turning of a titanium alloy. Measurement 151:107213. https://doi.org/10.1016/j.measurement.2019.107213
20. Veljkovic Z, Radojević S, Spasojević-Brkić VK (2019) From Taguchi's orthogonal arrays to full factorial designs and back. In Book: A closer look at loss function
21. Zhang L, Xu JI, Shuo S (2017) The study on high speed turning parameters optimization of TC21 titanium alloy. Acad J Manuf Eng 15(2):101–105
22. Zhang S, Liang Y, Xia Q, Ou M (2019) Study on tensile deformation behavior of TC21 titanium alloy. J Mater Eng Perform 28:1581–1590. https://doi.org/10.1007/s11665-019-03901-x
23. Yi SX, Yang ZJ, Xie HX (2022) Hot deformation and constitutive modeling of TC21 titanium alloy. Materials 15(5):1923. https://doi.org/10.3390/ma15051923
24. Qian X, Duan X (2020) Effect of tool microstructure on machining of titanium alloy TC21 based on simulation and experiment. Int J Adv Manuf Technol 111:2301–2309. https://doi.org/10.1007/s00170-020-06248-z
25. Zhang X, Wu H (2018) Effect of tool angle on cutting force and residual stress in the oblique cutting of TC21 alloy. Int J Adv Manuf Technol 98:791–797. https://doi.org/10.1007/s00170-018-2324-z
26. Wu H, To S (2015) Serrated chip formation and their adiabatic analysis by using the constitutive model of titanium alloy in high -speed cutting. J Alloys Compd 629:368–373
27. Wu H, Guo L (2014) Machinability of titanium alloy TC21 under orthogonal turning process. Mater Manuf Process 29(11–12):1441–1445. https://doi.org/10.1080/10426914.2014.952023
28. Pei L, Shu X (2021) Investigation of the turning process of the TC21 titanium alloy: experimental analysis and 3D simulation. Proc Inst Mech Eng Part E: J Process Mech Eng 235(2):489–498. https://doi.org/10.1177/0954408920967777
29. Zhang X, Wu H (2018) Effect of tool angle on cutting force and residual stress in the oblique cutting of TC21 alloy. Int J Adv Manuf Technol 98:791–797
30. Qian X, Duan X (2020) Effect of tool microstructure on machining of titanium alloy TC21 based on simulation and experiment. Int J Adv Manuf Technol 111:2301–2309
31. Muhammad R (2021) A fuzzy logic model for the analysis of ultrasonic vibration assisted turning and conventional turning of Ti-based alloy. Materials 14(21):6572. https://doi.org/10.3390/ma14216572
32. Muhammad R, Maurotto A, Roy A, Silberschmidt VV (2012) Ultrasonically assisted turning of Ti-6Al-2Sn-4Zr-6Mo. J Phys: Conf Series. https://doi.org/10.1088/1742-6596/382/1/012016
33. Maurotto A, Siemers C, Muhammad R, Roy A, Silberschmidt V (2014) Ti Alloy with Enhanced Machinability in UAT Turning. Metall and Mater Trans A 45:2768–2775
34. Che-Haron CH (2001) Tool life and surface integrity in turning titanium alloy. J Mater Process Technol 118(1–3):231–237
35. Singaravel B, Selvaraj T (2016) Application of Taguchi method for optimization of parameters in turning operation. J Manuf Sci Prod. https://doi.org/10.1515/jmsp-2016-0004
36. Athreya S, Venkatesh YD (2012) Application of Taguchi method for optimization of process parameters in improving the surface roughness of Lathe facing operation. Int Refer J Eng Sci 3:13–19
37. Athreya S, Venkatesh YD (2012) Application of Taguchi method for optimization of process parameters in improving the surface roughness of Lathe facing operation. Int Refer J Eng Sci 1:13–19
38. Tao SUN, Lufang QIN, Junming HOU, Yucan FU (2020) Machinability of damage-tolerant titanium alloy in orthogonal turn-milling. Front Mech Eng 15(3):504–515

Publisher's Note